

NASA
TN
D-5013
pt. 2,
c.1

NASA TECHNICAL NOTE



NASA TN D-5014

NASA TN D-5014



LOAN COPY: RETURN TO
AFWL (WLIL-2)
KIRTLAND AFB, N MEX

A 1-MEGAWATT REACTOR DESIGN FOR BRAYTON-CYCLE SPACE POWER APPLICATION

II - Neutronics Design

by Charles L. Whitmarsh, Jr., and Paul T. Kerwin

*Lewis Research Center
Cleveland, Ohio*



A 1-MEGAWATT REACTOR DESIGN FOR BRAYTON-CYCLE
SPACE POWER APPLICATION

II - NEUTRONICS DESIGN

By Charles L. Whitmarsh, Jr., and Paul T. Kerwin

Lewis Research Center
Cleveland, Ohio

NATIONAL AERONAUTICS AND SPACE ADMINISTRATION

For sale by the Clearinghouse for Federal Scientific and Technical Information
Springfield, Virginia 22151 - CFSTI price \$3.00

ABSTRACT

General characteristics were determined for a gas-cooled reactor designed to operate at 1 MW for 25 000 hours, with a coolant outlet temperature of 1650 K. Design curves relating core size to fuel concentration are presented as a function of radial power flattening.

A 1-MEGAWATT REACTOR DESIGN FOR BRAYTON-CYCLE

SPACE POWER APPLICATION

II - NEUTRONICS DESIGN

by Charles L. Whitmarsh, Jr., and Paul T. Kerwin

Lewis Research Center

SUMMARY

Neutronics design calculations were performed for a 1-megawatt thermal gas-cooled reactor required to operate for 25 000 hours with a coolant outlet temperature of 1650 K. The reactor model is a cylindrical core (length = diameter) contained in an 0.95-centimeter-thick tungsten pressure vessel. Core structural materials are tantalum, tungsten, and their alloys. The fuel is either enriched uranium dioxide or uranium nitride. Control is achieved by axial movement of beryllium oxide radial reflectors. The control range is a nominal 10 percent reactivity with a maximum multiplication constant of 1.05.

Design curves relating minimum core size to uranium concentration are generated for reactors reflected axially by a 1.27-centimeter-thick tungsten end plate and radially by a 7.62-centimeter-thick beryllium oxide reflector. These design curves include radial peak- to average-power ratios of 1.05, 1.10, and 1.35. In addition parametric data are presented such that design curves for other conditions can be calculated.

The radial power flattening (achieved by variation of fuel enrichment in annular zones) sufficiently enhanced reflector worth so that control is feasible inside an adjacent 4π shield. Spatial and energy flux distributions calculated for a representative configuration indicate that the median fission energy and prompt-neutron lifetime in the core are 0.35 MeV and 0.3 microsecond, respectively.

INTRODUCTION

Nuclear-reactor-powered Brayton-cycle systems are of interest for space applications requiring electric power in the range of tens of kilowatts to megawatts (refs. 1 and 2). The Brayton system has the advantages of a noncorrosive working fluid, high cycle

efficiency, and a relatively well-developed component technology; but it also has such disadvantages as large piping and components to be shielded and large radiator area. The application of this reactor system at high powers is generally restricted by radiator area.

Although either a liquid-metal-cooled or a gas-cooled reactor is useful as a heat source for Brayton systems, only gas-cooled reactors are considered herein. Such design goals as high-temperature operation and small core size have led to typical reactor characteristics of highly enriched, highly dense fuel, refractory-metal structural components, and reflector control systems (ref. 3). As a result the cores have high-energy flux spectrums and are categorized as "fast" reactors.

This study is of gas-cooled reactors for use in an "advanced-state-of-the-art" Brayton-cycle space power system. The objective is a preliminary reactor design that would produce 1 megawatt of thermal power for 25 000 hours with a turbine inlet temperature of 1650 K and that would retain all fission gases in the core. A single-loop system was selected so that the reactor coolant outlet temperature could be assumed to be equal to the turbine inlet temperature. The reactor core is composed of either fuel-pin bundles or a solid matrix fuel penetrated by coolant passages. Since reactor size with its associated shield weight penalty is of major importance to space power systems, design effort was concentrated on minimization of core size.

The design study is presented in two reports: I - THERMAL ANALYSIS AND CORE DESIGN, and II - NEUTRONICS DESIGN. Part I contains the heat-transfer and fluid-flow calculations required to define the internal core configuration and to show the effect of various design parameters on core size. Part II defines the general reactor configuration, the control system, and the materials of construction and presents core sizing data.

More specifically, this report, part II, NEUTRONICS DESIGN, shows the relation between core size and required fuel content for a range of nuclear design variables. The primary variables are reflector worth and radial power flattening. In addition, the neutron-flux spatial and energy distributions, the neutron lifetime, the control system, and the shield effects which are typical of this general class of reactors are presented.

REACTOR CONCEPT

A cycle analysis (ref. 4) for a one-loop Brayton-cycle system, which uses a 1-megawatt nuclear reactor heat source to supply 1650 K gas to a turbine, resulted in the recommended conditions shown in figure 1. For the cycle analysis the reactor was treated as merely a heat source with only the inlet and outlet conditions specified. For the neutronics analysis a cylindrical core with a length to diameter ratio (L/D) of 1 was selected because it provides (1) small critical core size, (2) good heat-transfer charac-

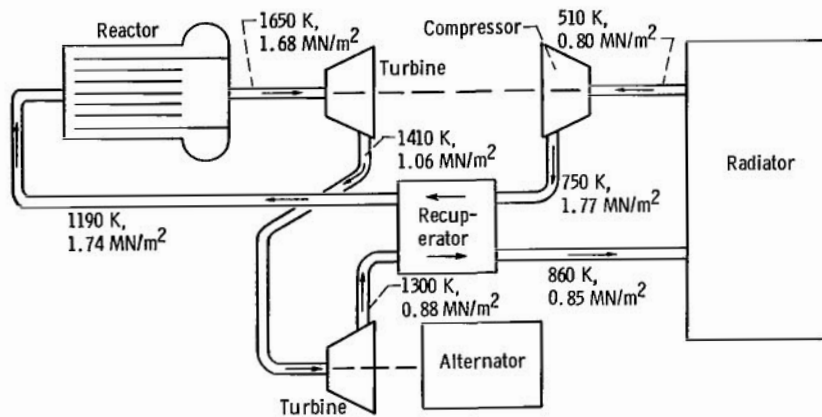


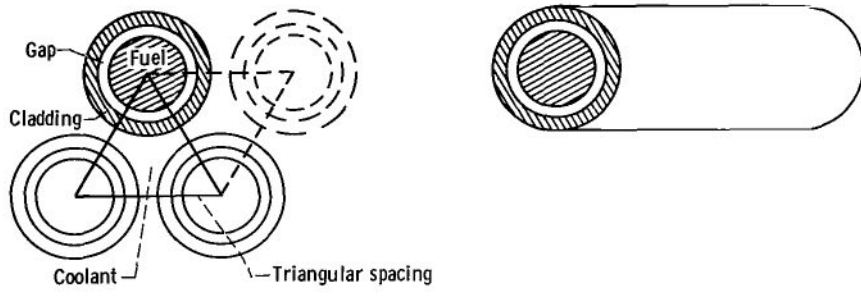
Figure 1. - Schematic drawing of Brayton-cycle system. Working fluid, 40 percent He - 60 percent Xe gas mixture (molecular weight = 80 kg/kg-mole); mass flow rate, 8.5 kilograms per second.

teristics, (3) ease of fabrication, and (4) application to either shadow or 4π shielding systems. The core could consist of either (1) bundles of fueled tubes with the coolant gas external to and flowing parallel to the tubes (pin core) or (2) a number of hexagonal fuel elements fitted together and penetrated by holes through which the coolant gas flows (matrix core). These concepts are illustrated in figures 2(a) and (b), respectively.

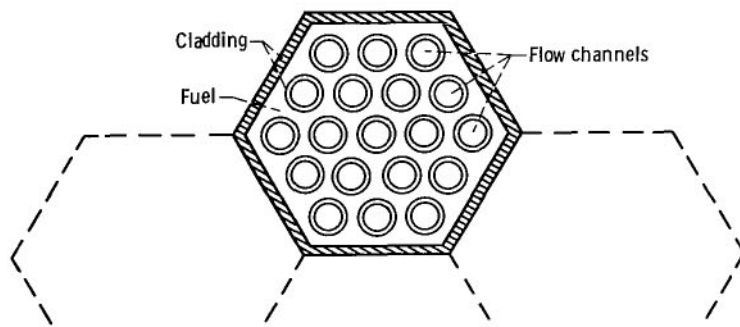
Two fuel arrangements in the core were considered, namely, uniform distribution of fully enriched fuel (93.2 percent U^{235}) and nonuniform distribution in which the core was divided into six radial zones with fuel enrichment varied among zones to achieve a flat power distribution (ref. 5). Space for the collection of fission gases is provided in the fuel pins but was not needed in matrix fuel elements. The core is contained in a pressure vessel and has end plates at both ends. Control is effected by a split radial reflector which forms a sheath around the core. Leakage of neutrons (and therefore reactivity control) can be regulated by axial movement of all or part of the reflector (fig. 3).

For a small core, an external control system is preferred, for example, reflector control. However, the particular method of operation (leakage control by axial movement) was chosen somewhat arbitrarily. A literature search (refs. 6 to 8) indicated that (1) radial reflectors could give sufficient reactivity changes by regulating core leakage, (2) end plates were effective as axial reflectors, (3) additional axial reflectors saved little in overall length (core plus reflector), and (4) heavy reflector materials were almost as effective per unit of thickness as light (moderating) materials.

The choice of materials is primarily dependent on the high-temperature (>1900 K) environment in the reactor. Selection of structural materials was thus limited to tungsten (W), tungsten - 25 percent rhenium alloy (W-25Re), and a tantalum-base alloy (ASTAR-811C) (ref. 9). Uranium dioxide (UO_2) (ref. 10), uranium nitride (UN) (ref. 11),



(a) Pin core designs.



(b) Matrix core designs.

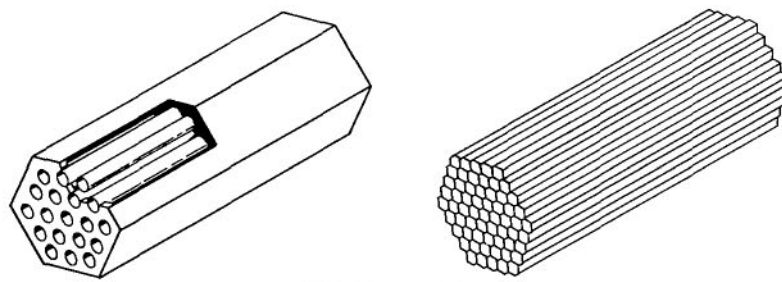


Figure 2. - Fuel-element configurations.

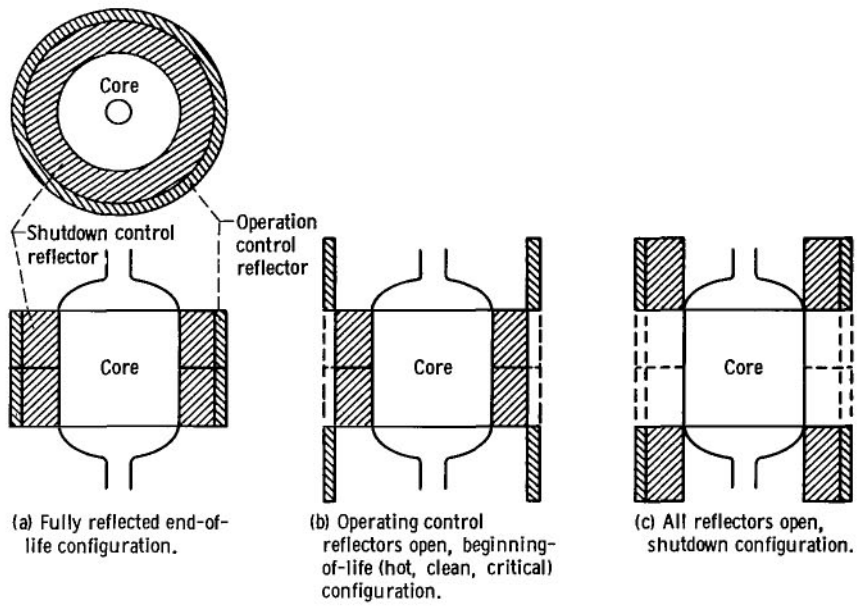


Figure 3. - Radial reflector configuration.

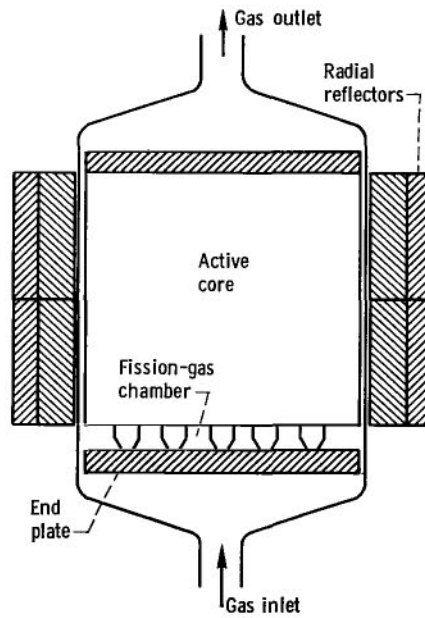


Figure 4. - Schematic drawing of gas-cooled, reflector-controlled, fast-spectrum reactor.

and a matrix of 60 volume percent UO_2 in W (ref. 12) were considered for reactor fuels. These materials have good high-temperature properties and high uranium concentration. In addition to having a high-temperature capability, the reflector material must also have a small neutron-absorption cross section for fast neutrons. Beryllium oxide (BeO) was selected over several applicable materials, such as molybdenum (Mo), niobium (Nb), or alumina (Al_2O_3) because of lower weight for equivalent reactivity worth. The reactor concept is shown in figure 4.

ANALYTICAL PROCEDURE

Calculational Model

Based on the concept developed in the preceding section, the geometric model shown in figure 5 was used in the reactor calculations. Only a quarter of a vertical cross-section is shown because the reactor configuration is symmetrical about the axial centerline and reactor midplane. The same model was applicable to either the pin or

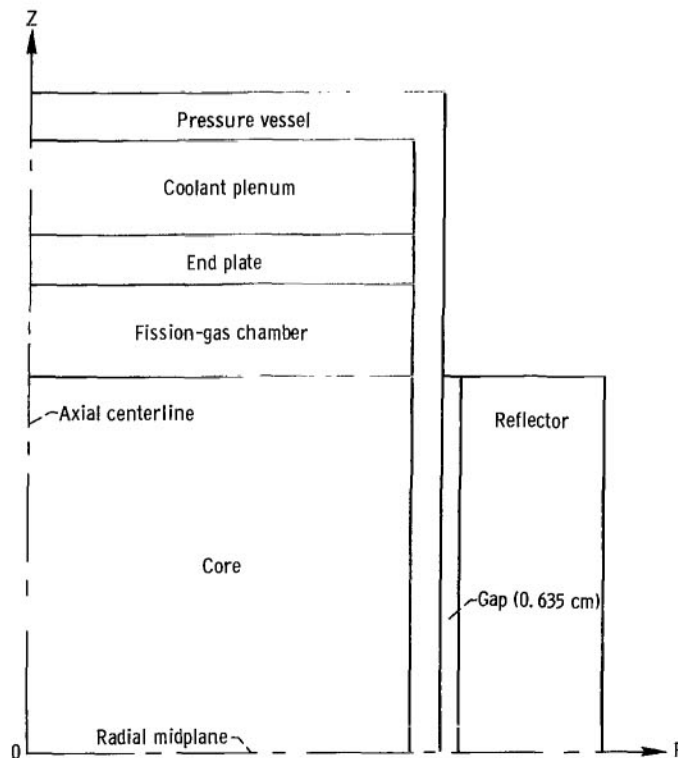


Figure 5. - Neutronics calculation model.

the matrix core calculations because the core region was assumed to be homogenized. This assumption permits use of one-dimensional calculation methods and is an accurate assumption when neutron mean free paths are large compared with region dimensions. The complete absence of any in-core moderating materials indicates that all designs will have a high-energy neutron spectrum, which in turn means that neutron mean free paths will be relatively large (>2 cm).

Criticality Calculations

The anticipated small core size (diameter of 30 to 40 cm) and fast-neutron spectrum led to the use of the multigroup transport codes DTF (ref. 13) and TDSN (ref. 14). A set of 16-group spectra-averaged cross sections was generated with the GAM-II (ref. 15) and TEMPEST-II (ref. 16) codes. Cross sections and code options were verified by calculations of critical experiments with similar materials and configurations (see appendix A).

Reactivity Calculations

Design changes, for example, a change in reflector thickness, can be represented by changes in reactivity. To be useful as parametric design data, these reactivity effects should be both independent of each other when more than one design change is made on the same system and applicable to a noncritical system. The reactivity equations utilized in this report are as follows:

$$\Delta\rho_i = \frac{k_2 - k_1}{k_2 k_1} \times 100 \quad (1)$$

$$\Delta\rho_{\text{total}} = \sum_{i=1}^N \Delta\rho_i \quad (2)$$

where $\Delta\rho_i$ is the i^{th} component of the total percent reactivity change (or reactivity worth), k_1 is the multiplication constant of the initial reactor, and k_2 is the multiplication constant of the perturbed reactor as derived from perturbation theory. Thus, the results are subject to the same assumptions and limitations as perturbation theory (ref. 17). The more important limitation is that the flux energy spectrum is

assumed to be constant from the initial to the perturbed state. Accuracy, therefore, diminishes with increasing deviation from criticality ($k = 1$).

RESULTS

Criticality

Because most nonfissile reactor materials have similar fast-neutron cross sections, criticality calculations are somewhat insensitive to small changes in composition. Thus, parametric calculations based on cores with nominal compositions (void volume fractions f_v of 0.15 and cladding- to fuel-volume-fraction ratios f_c/f_f of 0.1 to 1.0) may be used for general core sizing. The relation between U^{235} density in the core and the multiplication constant for cylindrical, "bare" cores with $L/D = 1$ and diameters of 29 to 42.7 centimeters is shown in figure 6. Bare core is used here to denote an unreflected core surrounded radially by a 0.95-centimeter-thick tungsten pressure vessel. All calculations were based on fully enriched (93.2 percent U^{235}) UO_2 or UN fuel with either ASTAR-811C or W-25Re as the fuel cladding material.

Although pressure vessel thickness generally is dependent on diameter, use of a constant thickness for neutronics calculations appears justified. In a fast-spectrum reactor, the pressure vessel acts more as a reflector than an absorber, and since its

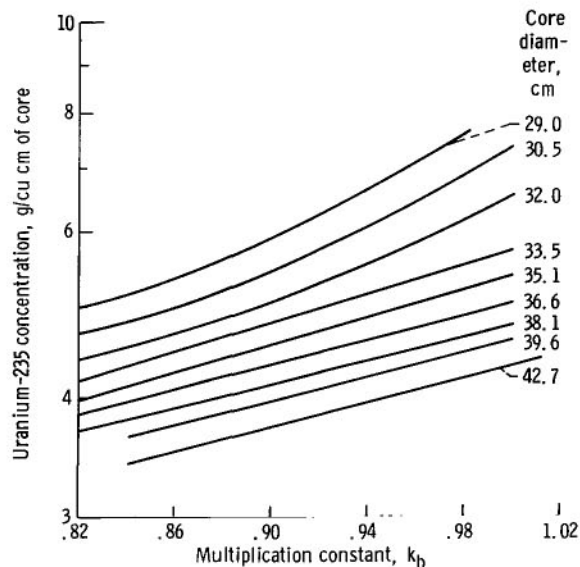


Figure 6. - Multiplication constant as function of uranium-235 concentration for unreflected, cylindrical, fast-spectrum reactor. Pressure vessel, 0.95-centimeter tungsten; length to diameter ratio, 1.

thickness is small compared with the actual reflector, the multiplication constant is insensitive to small changes in pressure vessel thickness. A value of about 1 percent Δk gain per centimeter increase in thickness was calculated for a tungsten pressure vessel.

Control System

Reactivity requirements. - The reactivity required for reactor operation can be classified into four categories: (1) fuel burnup, (2) Doppler effect, (3) temperature effect, and (4) shutdown margin.

Fuel burnup was calculated from the design specifications of 25 000 hours operation at 1 megawatt as follows:

$$\text{Burnup} = \text{Power} \times \text{Time}$$

or

$$B_T = 10^6 \text{ watts} \times 3.1 \times 10^{10} \frac{\text{fissions}}{\text{watt-sec}} \times \frac{235 \text{ g U}^{235}}{\text{mole}} \times \frac{1 \text{ mole}}{6.023 \times 10^{23} \text{ atoms U}^{235}} \times \frac{1 \text{ atom}}{\text{fission}} \times 9 \times 10^7 \text{ sec} \quad (3)$$

$$B_T = 1100 \text{ g U}^{235}$$

For the critical masses anticipated in this study, 1.1 kg of U^{235} represents about 0.5 to 1 percent of the inventory of large and small cores, respectively. This fuel loss represents a reactivity change of about 0.5 percent (see fig. 6). Because of the smallness of the reactivity change, a more detailed calculation including fission-product buildup was considered unnecessary. Thus, a nominal 1 percent reactivity allowance was provided for fuel burnup.

Calculations of Doppler coefficient were not attempted because accurate values are difficult to obtain for fast, highly enriched reactors and are therefore considered beyond the scope of a parametric study such as this. The Doppler coefficient probably is negative but sufficiently small (ref. 18) that zero was assumed. Approximate calculations indicated values near -0.1 percent reactivity for small cores and -0.5 percent reactivity for large cores.

The temperature effect represents the change of reactivity from the cold-clean con-

dition to full-power operation resulting from material density and core geometry changes. Criticality calculations on a representative core ($D = 32.6$ cm, $f_f = 0.72$, $f_c = 0.073$) indicated a loss of ~ 1.8 percent reactivity because of these changes. These calculations were based on estimated average operating temperatures of 1720 K for the fuel, 1520 K for the cladding and pressure vessel, and 1250 K for the reflector. Homogenized cores were used in the calculation and therefore detailed geometric effects within the core were not considered. However, expansion of the reflector and change in core length were included in the calculation.

The amount of subcritical reactivity needed for shutdown margin is primarily a matter of the safety and hazards analysis and is dependent on the application. One criterion which seems reasonable for this study is that with half the control system in the "in" position, the cold-clean core should be subcritical. Thus, if a 2.2 percent reactivity contingency is added to the temperature and burnup reactivity requirements, a shutdown margin of about 5 percent reactivity is required. It follows that the design multiplication factor will be 1.05 and the total control range of the reflectors must be greater than 10 percent reactivity (table I).

TABLE I. - REACTIVITY CONTROL
REQUIREMENTS

Category	Nominal reactivity needed, percent
Fuel burnup	1.0
Doppler	---
Temperature defect	1.8
Contingency	2.2
Shutdown	5.0
Total	10.0

Reflector worth. - For a given core diameter, reactivity worth of the reflector increases with increasing reflector thickness, as shown in figure 7. However, the rate of increase lessens as reflector thickness increases. For a fixed reflector thickness, reactivity worth decreases with increasing core diameter. These data represent criticality calculations for uniformly fueled cores surrounded by a 0.95-centimeter-thick tungsten pressure vessel both with and without a radial reflector. Also shown in figure 7 is a relative increase in reflector worth of 0.5 (about 6 percent reactivity) for a

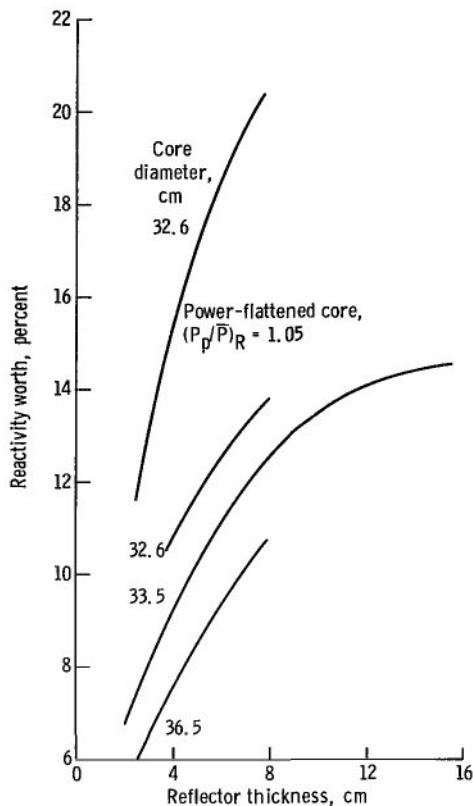


Figure 7. - Reactivity worth of radial BeO reflectors surrounding cylindrical, fast-spectrum reactor core. Fuel, UO_2 ; cladding, ASTAR-811C; pressure vessel, 0.95-centimeter tungsten; length to diameter ratio, 1.

32.6-centimeter-diameter core when fuel enrichment is varied in annular zones to obtain a radial peak-to-average power ratio $(P_p/\bar{P})_R$ of 1.05 (case II, ref. 5).

Thus, the minimal control requirement of about 10 percent reactivity should be obtainable for uniformly fueled cores less than 34 centimeters in diameter with a radial BeO reflector greater than 5 centimeters thick. Larger cores would require thicker reflectors. Operating control of 1.0 percent reactivity required to compensate for fuel burnup over the core life could be regulated by moving the outer 2 centimeters of the reflectors of an unzoned core and the outer centimeter for a zoned core.

The reactivity worth of a radial reflector as a function of core diameter is shown in figure 8. These results were calculated for uniformly fueled, fully enriched cores with different compositions, although all had a 7.62-centimeter BeO radial reflector.

The effect of axial reflection was simulated by varying the thickness of the tungsten end plates. Symmetric configurations with the same thickness of tungsten at each end of

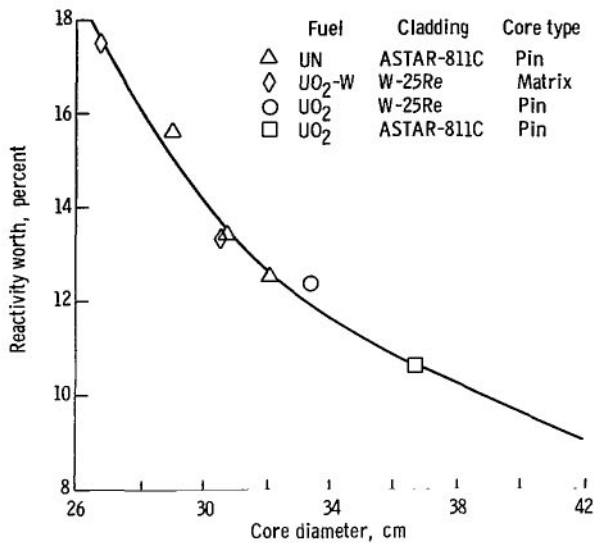


Figure 8. - Reactivity worth of 7.62-centimeter BeO radial reflector surrounding cylindrical, uniformly fueled, fast reactor core with length to diameter ratio of 1.

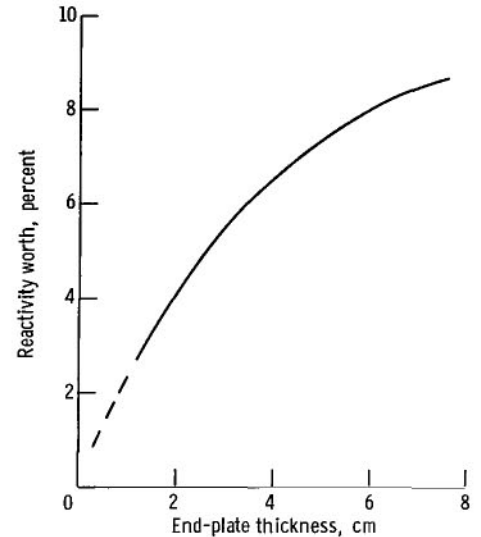


Figure 9. - Reactivity worth of tungsten end plates in BeO reflected, fast-spectrum, cylindrical reactor core. End plate, 80 percent W - 20 percent void; fuel, UO₂; cladding, ASTAR-811C; pressure vessel, 0.95-centimeter tungsten; length to diameter ratio, 1; 7.62-centimeter BeO radial reflector.

the core were considered, and the tungsten density was reduced 20 percent to account for coolant passages. The shape of the reactivity-worth curve was similar to the one for the BeO radial reflectors although the worth per unit thickness was less (fig. 9). The qualitative results of radial and axial reflectors should be the same, that is, decreased worth with increased core size at constant length to diameter ratio. However, calculations indicated axial reflector worths to be relatively insensitive to such changes. For a core-diameter change from 30 to 42 centimeters, the change in worth of the 1.27-centimeter tungsten axial reflector was less than 0.6 percent reactivity. The effect on axial reflector worth of changing radial reflector thickness from 7.62 centimeters to 5.08 centimeters on a 32.6-centimeter-diameter core was calculated to be of similar magnitude. Therefore, a single curve (fig. 9) was used to determine axial reflector worth for all core configurations considered in this study.

The final determination of end-plate thickness will probably depend on fabrication considerations rather than reactivity. With this in mind, a value of 1.27 centimeters was selected in this parametric study for the reference design calculations.

A comparison of radial reflector worths of different materials showed that, for a reflector thickness of 6.35 centimeters, the moderating material BeO is worth 3 to 4 percent more reactivity than the nonmoderating materials Mo or Nb (table II). Part of this increase was due to the greater $n-2n$ reaction in Be, which indicates that the reflection properties per unit thickness of these materials are nearly equal.

Shield effect. - Leakage-controlled fast reactors are inherently sensitive to any

TABLE II. - EFFECT OF REFLECTOR MATERIAL ON REACTIVITY WORTH OF 6.35-CENTIMETER RADIAL REFLECTOR ON SMALL, ZONED-CORE, FAST-SPECTRUM REACTOR

Reflector material	Reactivity worth	
	Percent	Relative
BeO	19	1.0
Mo	16	.84
Nb	15	.79

TABLE III. - EFFECT OF INFINITELY THICK TUNGSTEN SHELL (4π SHIELD) ON UNZONED FAST-SPECTRUM REACTOR REFLECTED WITH 7.62 CENTIMETERS OF BeO

Distance from outer surface of reflector, cm	Control range with 7.62-cm BeO shell, percent reactivity	Center- to average-power ratio
(No shield)	22	1.41
30.5	19	1.38
15.2	17	1.37
0	7.6	(a)

^aNot calculated but should be about 1.37.

material external to the reactor system since this material acts as a neutron reflector. The effect of shield material on the reflector control range was therefore investigated because application of these reactor systems would require shielding. Since specific shielding requirements are unknown, this investigation was both general and brief.

Results presented in table III indicate the reactivity control range of a 7.62-centimeter BeO reflector when an infinitely thick tungsten 4π shield is placed at various distances from the outer edge of the reflector. The two extreme positions, no shield and an adjacent shield, show a difference of 14 percent reactivity in the control range of a 7.62-centimeter BeO reflector. Other effects noted were an increase of multiplication constant k and a reduction of the center- to average-power ratio from 1.41 to 1.37.

These results are based on a spherical reactor with an 18.5-centimeter-diameter core surrounded by a 0.95-centimeter-thick tungsten pressure vessel and a 7.62-centimeter BeO reflector. Therefore, these results are only qualitative, and the trends are applicable to cylindrical systems with radial reflectors.

Since the control range of an unzoned spherical core with an adjacent shield was less than the nominal 10 percent reactivity required in this study, a more specific calculation was performed. The reflector control range of a reference-design core (33.5-cm-diam cylindrical core with $L/D = 1$, radially zoned to $(P_p/\bar{P})_R = 1.05$, a 7.62-cm-thick BeO radial reflector, and $k = 1.05$) was calculated to be 8.4 percent reactivity with an infinite tungsten shield adjacent to the BeO radial reflector. This value is sufficiently close to the 10 percent reactivity nominal control requirement to indicate design feasibility. However, other factors are involved which would require a redesign of the core for operation inside a shield. The reference core power ratio $(P_p/\bar{P})_R$ increased to

1.12 in the peripheral fuel zone and the design k increased to 1.089. These two effects on core size are opposing, and the net result is unknown without additional calculations. For this study the additional design effort was considered unwarranted, and it should suffice to say that operation with an adjacent shield appears feasible.

Power Distribution

The radial power distribution calculated for a uniformly fueled, fully enriched reactor with a BeO radial reflector is presented in figure 10. The local- to average-power ratio, which peaks at the core center, decreased from 1.42 to 1.28 as the radial reflector thickness was increased from 5.08 to 7.62 centimeters. These reflector thicknesses represent probable initial and end-of-life positions. There was no indication of power peaking at the core-reflector interface. This design problem is often encountered when a fast core is adjacent to a moderating medium since high-energy neutrons that escape from the core and return at lower energies are immediately absorbed by the dense fuel material. Because of anticipated materials problems related to fission-gas retention in core regions with relatively high power output (ref. 4), power flattening by variation of fuel enrichment in radial core zones was considered. The neutronics aspects of power flattening were reported previously (ref. 5) and are summarized as follows.

Power flattening by variation of fuel enrichment perturbs the reactivity of a fully enriched, uniformly fueled reactor in two ways:

- (1) Reactivity is reduced because fuel (U^{235}) must be removed.

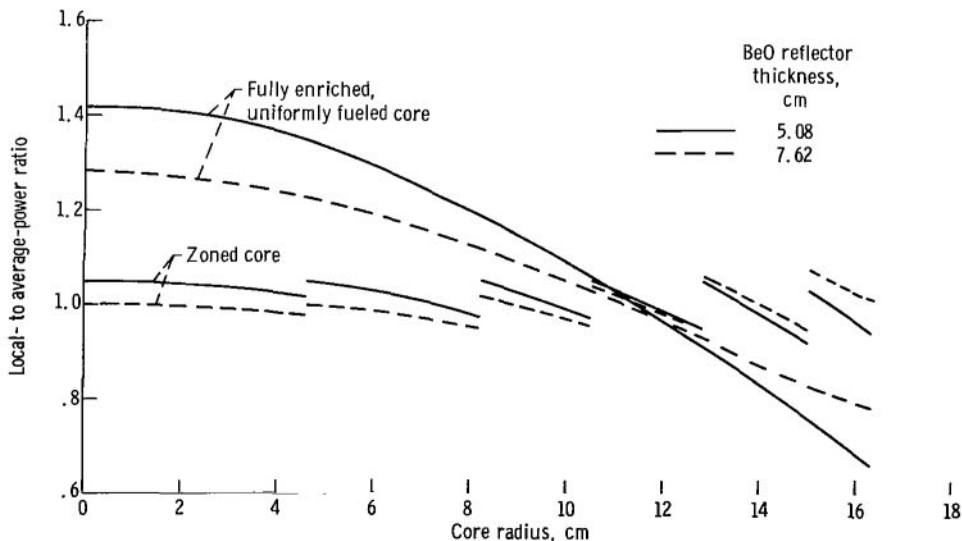


Figure 10. - Radial power profiles in zoned and unzoned fast-spectrum reactors with BeO radial reflectors.

TABLE IV. - REACTIVITY COST TO RADIAL POWDER FLATTEN
CYLINDRICAL, REFLECTOR-CONTROLLED, FAST-SPECTRUM
REACTOR WITH 32.6-CENTIMETER DIAMETER AND LENGTH

[Radial BeO reflector thickness, 5.08 cm.]

Radial peak- to average-power ratio, $(P_p/\bar{P})_R$	Reactivity			
	Loss from U^{235} removal, percent	Gain from increased reflector worth		Net loss, percent
		Percent	Relative	
1.05	12	6	1.5	6
1.10	5	2	1.15	3

(2) Reactivity is increased because the worth of the radial reflector is increased. Reactivity values for these items based on a representative core design are listed in table IV. This design assumes that shutdown control will be achieved by a 5.08-centimeter BeO radial reflector and operating control by an additional 2.54 centimeters of BeO. The peak- to average-power ratios of 1.05 and 1.10 were estimated to be lower limits that could be reasonably obtained by fuel zoning. Thus, the reactivity cost to zone to a $(P_p/\bar{P})_R$ of 1.05 was 6 percent and to a $(P_p/\bar{P})_R$ of 1.1 was 3 percent.

These data are indicative of the initial (beginning of life) core configuration only, with the shutdown reflector closed and the operating control reflector open. The resulting distortion of the radial power shape caused by reflector movement to compensate for fuel burnup over the core life was calculated for an operating reflector thickness of 2.54 centimeters. This nominal thickness was selected in the initial stage of the study and therefore does not coincide with the outer 1 centimeter indicated in the section Reflector worth. However, any effects of this difference in reflector thickness on the final core design are considered to be small.

The data in table V (and fig. 10) indicate that the $(P_p/\bar{P})_R$ in the two peripheral zones exceeds 1.05 in the fully reflected (7.62 cm) configuration. However, for some design calculations, such as fission-gas production, the quantity of interest is the time-averaged (or "effective") value of $(P_p/\bar{P})_R$. If the operating reflector is assumed to be withdrawn at the beginning of core life and inserted at the end of core life and its movement is assumed to be linear with fuel burnup, the effective value for $(P_p/\bar{P})_R$ is then about 1.05 and occurs in the outer two zones.

An alternate power-flattening method is to use a fuel distribution which would provide a $(P_p/\bar{P})_R$ of 1.05 for the end-of-life configuration (7.62-cm BeO radial reflector). Data presented in reference 5 show that, although the reactivity penalty would be less

TABLE V. - DISTORTION OF RADIAL POWER SHAPE IN ZONED-CORE,
FAST-SPECTRUM REACTOR CAUSED BY CHANGING

REFLECTOR THICKNESS

Radial zone	Enrichment, percentage of U^{235}	Initial reflector configuration, 5.08 centimeters BeO	End-of-life reflector configuration ^a , 7.62 centimeters BeO
		Radial peak- to average-power ratio, $(P_p/\bar{P})_R$	
1 (central)	57.9	1.05	1.00
2	60.2	↓	1.00
3	65.8		1.02
4	71.8		1.04
5	81.0		1.06
6 (peripheral)	93.2	1.03	1.08

^aZero fuel depletion was considered in the calculation. An estimated value of 1.09 would occur in the peripheral zone if 25 000-MW-hr burnup were considered.

(3 percent compared with 6 percent), power distortion over the core lifetime would be greater. For example, the central zone would have an initial $(P_p/\bar{P})_R$ of 1.10 and a final value of 1.05, with the effective (or average) ratio being greater than 1.05. Therefore, this method was judged to be less desirable.

The axial power distribution was calculated to be of a shape that could be approximated by $\cos \pi Z/Le$ where Le/L , the ratio of extrapolated length to actual length, was dependent on the end-plate thickness (table VI). For a thickness range of zero to 7.62 centimeters, Le/L varied from 1.15 to 1.56 and the axial peak- to average-power ratio $(P_p/\bar{P})_Z$ varied from 1.37 to 1.19. For the selected thickness of 1.27 centimeters, the corresponding values were 1.31 for $(P_p/\bar{P})_Z$ and 1.27 for Le/L . Although the symmetric cosine function was used throughout this study to represent the axial power distribution, it was recognized that from the standpoint of heat transfer this was not the best shape. A nonsymmetrical distribution with its maximum near the core inlet would increase the average temperature difference between fuel and coolant. This heat-transfer benefit associated with the axial fuel zoning was considered to be offset by the calculational and fabrication complexities. Therefore, no axial power flattening was attempted.

TABLE VI. - AXIAL POWER DISTRIBUTION^a IN
SMALL, FAST-SPECTRUM REACTOR

Case	Tungsten end-plate thickness ^b , cm	Axial peak- to average-power ratio, $\left(\frac{P_p}{\bar{P}}\right)_Z$	Ratio of extrapolated length to active fuel length, Le/L ^c
1	0	1.37	1.15
^d 2	1.27	1.31	1.27
3	2.54	1.27	1.35
4	5.08	1.22	1.48
5	7.62	1.19	1.56

^aBased on one-dimensional calculations with radial reflection approximated by reflector savings.

^bAxial symmetry with end plate located at each end of core.

^cCalculated value which fits the power distribution to a chopped cosine shape, $\pi Z/Le$.

^dChecked with two-dimensional calculation with 7.62-cm BeO radial reflector.

Design Correlation

If the assumption is made that the various reactivity effects considered herein are both independent of each other and of the multiplication level of the core, these effects can be combined in a general design correlation of bare-core size to the design parameters (e. g., end-plate thickness, radial reflector thickness, and radial fuel zoning to attain power flattening). Thus,

$$\Delta\rho_{\text{total}} = (\beta + \delta) \eta + \gamma + \mu \quad (5)$$

where

β reactivity worth of 7.62-cm BeO radial reflector on uniformly fueled, fully enriched core (fig. 8)

δ change in reactivity worth for BeO radial reflector other than 7.62 cm (fig. 7)

η relative increase in reflector worth caused by radial fuel zoning (table IV)

γ reactivity worth of W end plates (fig. 9)

μ reactivity effect due to fuel removal caused by radial fuel zoning (table IV)

Then, based on a required multiplication factor of 1.05,

$$\Delta\rho_{\text{total}} = \frac{1.05 - k_b}{1.05 k_b} \quad (6)$$

where k_b is the bare-core multiplication factor (fig. 6). Also included in this formulation is the assumption that certain power-flattening effects are independent of core diameter (e.g., the relative increase of reflector worth and the reactivity lost by fuel removal).

Equation (6), then, is a correlation relating bare-core size to required fuel concentration for a particular set of design conditions. These data are presented in figure 11 for the recommended conditions of a 7.62-centimeter BeO radial reflector and 1.27-centimeter W end plates and for three degrees of radial power flattening ($(P_p/\bar{P})_R = 1.35, 1.10, \text{ and } 1.05$). Figure 11 represents the relation of fuel concentration to minimum

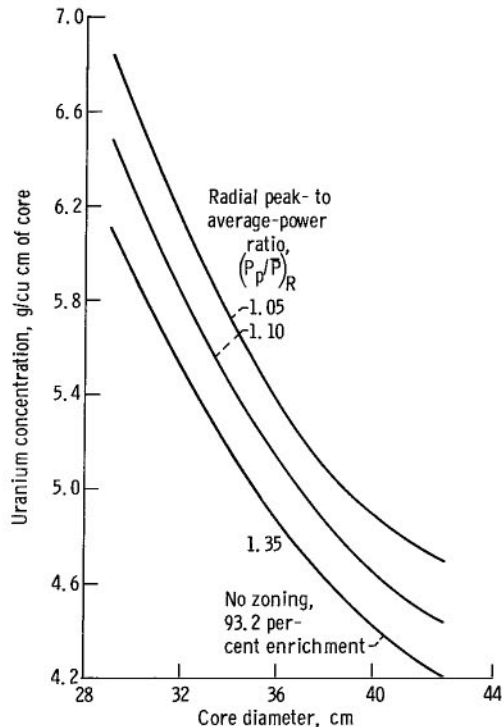


Figure 11. - Criticality design curves for fast-spectrum, gas-cooled, reflector-controlled reactor with radial peak-to-average-power ratios of 1.05, 1.10, and 1.35. Cylindrical core; fuel, enriched uranium; cladding, W-25Re; pressure vessel, 0.95-centimeter tungsten; length to diameter ratio, 1; axial reflector, 1.27-centimeter tungsten; radial reflector, 7.62-centimeter BeO; multiplication constant, k , 1.05.

core size for a gas-cooled reactor designed to operate at 1 megawatt for 25 000 hours with a coolant outlet temperature of 1650 K. Such a reactor would have the same reflector and pressure vessel configuration described in the preceding paragraph. It should be noted that the data in figure 11 represent the optimization (minimum core size) of a reactor (core plus control system) to perform a specific job. Thus, the correlation includes the interrelating effects of the reflector, core, and fuel.

If curves of uranium concentration against core diameter for other combinations of reflector thicknesses should be desired, these could be generated by substituting the appropriate reactivities from equation (5) into equation (6) to obtain the required bare-core multiplication factor k_p , from which the corresponding fuel density is obtained from figure 6. However, application of the parametric data to reactors with other than 7.62-centimeter BeO reflectors ($\delta \neq 0$) is probably limited to the unzoned core configuration (no radial power flattening). This procedure also requires the assumption that the increase in reflector worth per unit thickness is independent of core diameter. This is not rigorous, but the slope of the reactivity-worth curve between reflector thicknesses of 5 and 7.6 centimeters appears to be relatively insensitive to diameter change (fig. 7).

When using equations (5) and (6) to construct design curves, the term $(\beta + \delta)\eta$ must be greater than 10 percent to ensure shutdown margin, and the fuel damage from burnup must be evaluated. For the core-size range in figure 11, maximum burnup values for UO_2 fuel were calculated to be 4.7×10^{20} , 3.6×10^{20} , and 3.2×10^{20} fissions per cubic centimeter for the radial power ratios of 1.35, 1.1, and 1.05, respectively; and for UN fuel to be 6.1×10^{20} , 4.6×10^{20} , and 4.2×10^{20} fissions per cubic centimeter.

Core Characteristics

Flux spectra. - Flux spectra, calculated at various radial positions in a representative zoned core with a 7.62-centimeter BeO reflector indicated that even in the reflector the spectrum was still quite fast (fig. 12). Thermalized neutrons were essentially nonexistent; even near the outer edge of the reflector the calculated thermal- to total-flux ratio (ϕ_{th}/ϕ_{tot}) was 5×10^{-4} . Mean neutron flux energy varied from 0.41 MeV at the core center to 0.07 MeV at the outer edge of the reflector, and thus indicated some softening of the spectrum. Spectral data are summarized in table VII. The median fission energy in the core was calculated to be 0.35 MeV. Data on the spatial distribution of the flux, summarized in table VIII, indicate a leakage flux of 4×10^{13} neutrons per square centimeter per second.

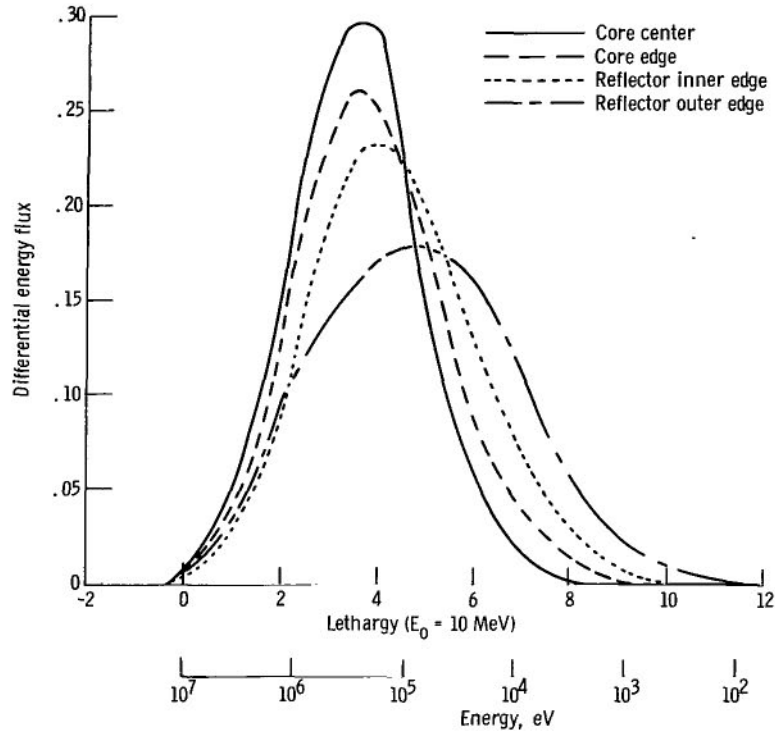


Figure 12. - Flux spectra in cylindrical, fast-spectrum reactor with 7.62-centimeter BeO radial reflector. (All spectra at core midplane.)

Neutron generation time. - A neutron generation time, or prompt-neutron lifetime, of about 0.3 microsecond was calculated for a representative power-flattened core using the α option in the DTF code. This technique is essentially the addition of an equivalent $1/v$ absorber to the core followed by a k calculation. The neutron generation time l_p for small $\Delta k/k$ could then be calculated by

$$l_p = \frac{\Delta k}{\alpha} \quad (4)$$

where

$$\frac{\Delta k}{k} = \frac{k - k_v}{k k_v}$$

and

k multiplication constant of core

k_v multiplication constant of core with $1/v$ absorber

α reciprocal reactor period, sec^{-1}

No neutron lifetime data on a similar system were available for comparison to check the calculated value. However, small, fast, bare cores have neutron lifetimes of the

TABLE VII. - NEUTRON FLUX SPECTRA IN BeO REFLECTED FAST-SPECTRUM REACTOR^a

Energy range	Core center		Core edge		Inside edge of reflector		Outside edge of reflector	
	Fraction of neutrons ^b	Flux per unit lethargy	Fraction of neutrons ^b	Flux per unit lethargy	Fraction of neutrons ^b	Flux per unit lethargy	Fraction of neutrons ^b	Flux per unit lethargy
3.7 to 15 MeV	0.0421	0.0301	0.0341	0.0244	0.0222	0.0159	0.0234	0.0167
0.82 to 3.7 MeV	.282	.188	.234	.156	.176	.117	.136	.0907
0.3 to 0.82 MeV	.297	.297	.256	.256	.225	.225	.123	.123
0.11 to 0.3 MeV	.236	.236	.223	.223	.221	.221	.154	.154
0.025 to 0.11 MeV	.125	.0833	.180	.120	.222	.148	.242	.161
5.5 to 25 keV	.0166	.0107	.0608	.0405	.0972	.0648	.180	.120
1.2 to 5.5 keV	9.2×10^{-4}	6.1×10^{-4}	.0105	.0070	.0261	.0174	.0860	.0573
0.28 to 1.2 keV	7.7×10^{-6}	5.1×10^{-6}	.0011	7.3×10^{-4}	.0069	.0046	.0317	.0211
0.1 to 0.28 keV	4.6×10^{-8}	4.6×10^{-8}	1.4×10^{-4}	1.4	.0017	.0017	.0100	.0100
0.03 to 0.1 keV	Small	Small	2.0	1.7	7.9×10^{-4}	6.6×10^{-4}	.0052	.0043
11 to 30 eV	↓	↓	Small	Small	3.9	3.9	.0023	.0023
3 to 11 eV	↓	↓	↓	↓	2.6	2.1	.0017	.0013
0.88 to 3 eV	↓	↓	↓	↓	3.7	3.0	.0015	.0012
0.41 to 0.88 eV	↓	↓	↓	↓	2.5	3.3×10^{-5}	4.3×10^{-4}	5.7×10^{-4}
0.1 to 0.41 eV	↓	↓	↓	↓	9.5×10^{-6}	6.7×10^{-6}	1.5	1.1
Thermal (<0.1)	↓	↓	↓	↓	5.9×10^{-5}	-----	4.8	-----
Median energy, MeV	0.41		0.32		0.22		0.075	

^aCalculated at midplane of 32.6-cm-diam zoned core surrounded radially by 0.95-cm tungsten pressure vessel at 7.62-cm BeO reflector.

^bNormalized to $\int_0^{15 \text{ MeV}} \phi(E) dE = 1$.

TABLE VIII. - SPATIAL FLUX DISTRIBUTION IN BeO REFLECTED FAST-SPECTRUM REACTOR

[Zoned core; 7.62-cm BeO radial reflector; 1.27-cm W end plate; 0.95-cm W pressure vessel.]

Fraction of neutrons absorbed	0.67
Fraction of neutrons leaking axially	0.13
Fraction of neutrons leaking radially	0.20
Flux at core center, neutrons/(cm ²)(sec)	8×10^{13}
Flux at core edge (radial), neutrons/(cm ²)(sec)	4×10^{13}

TABLE IX. - TYPICAL REACTOR CHARACTERISTICS^a

Power, MW	1
Core life, hr	25 000
Coolant	He-60 Xe
Coolant outlet temperature, K	1650
Coolant pressure, MN/m ²	1.71
Structural materials	W and W-25Re
Fuel material	U ²³⁵ O ₂ or U ²³⁵ N
Radial reflectors, cm of BeO	7.62
Axial reflectors (end plates), cm of W	1.27
Radial peak- to average-power ratio, $\left(\frac{P_p}{\bar{P}}\right)_R$	1.05, 1.10, or 1.35
Axial peak- to average-power ratio, $\left(\frac{P_p}{\bar{P}}\right)_Z$	1.31
Reactivity control range (unshielded), percent	>10
Maximum multiplication constant	1.05
Reactivity shutdown margin, percent	>5
Mean fission energy, MeV	0.35
Prompt-neutron lifetime, μsec	0.3
Flux core center, neutrons/(cm ²)(sec)	8×10^{13}
Leakage flux, neutrons/(cm ²)(sec)	4×10^{13}

^aRight-cylinder reactor core with length to diameter ratio of 1.0.

order of 0.02 microsecond (ref. 19), and small fast cores with thick Be reflectors have neutron lifetimes of about 5 microseconds (ref. 20). Thus, the calculated value of 0.3 microsecond for a fast core with an intermediate BeO-reflector thickness appears reasonable.

Typical Reactor Properties

The results of this study have indicated that a typical reactor design would have the properties summarized in table IX.

SUMMARY OF RESULTS

A model was conceived for a gas-cooled, compact nuclear reactor required to operate at 1 megawatt for 25 000 hours with a coolant outlet temperature of 1650 K. This

model has the following characteristics:

- (1) A cylindrical core with a length to diameter ratio of 1 surrounded by a 0.95-centimeter-thick pressure vessel, axial end plates, and a radial reflector
- (2) A control system based on neutron leakage and regulated by axial movement of a radial reflector
- (3) The materials $U^{235}O_2$ or $U^{235}N$ for fuel, W and W-25Re for structural components, and BeO for reflector

An analytical study of this reactor produced the following information:

1. A nominal control range of 10 percent reactivity was required based on (a) calculated reactivity values of 1 percent for fuel burnup and 1.8 percent for temperature effect, (b) an estimated 2.2 percent reactivity for contingency, (c) an assumed zero Doppler coefficient, and (d) 5 percent reactivity for shutdown margin. Thus, the multiplication constant for the reactor in the fully reflected condition is 1.05.

2. Reactivity worth of the radial reflector was shown to be a function of core diameter, reflector thickness, reflector material, and radial power distribution. For uniformly fueled, fully enriched cores with diameters less than or equal to 38 centimeters a BeO reflector greater than or equal to 7.6 centimeters does provide sufficient reactivity control range. The reflector worth for a 32.6-centimeter-diameter core with a 7.62-centimeter-thick reflector increased by a factor of 1.5 when the radial power distribution was flattened by fuel enrichment variation to a peak- to average-power ratio of 1.05. Reflector worths were decreased to relative values of about 0.8 when a 7.62-centimeter BeO reflector was replaced by the nonmoderating materials Nb or Mo.

3. A total BeO radial reflector thickness of 7.62 centimeters was selected for this study. The reflector was divided into two sections, the inner section for shutdown control and an outer section for operating control.

4. For the selected end-plate thickness of 1.27 centimeters, the calculated axial power distribution could be approximated by the function $\cos \pi Z/1.27 L$ which has a peak- to average-power ratio of 1.31.

5. Calculations indicate that sufficient reactivity control range with a 7.62-centimeter BeO radial reflector is available when a 4π tungsten shield is placed adjacent to the reflector of a core zoned to a $(P_p/\bar{P})_R$ of 1.05. However, the effects on core design were not determined.

6. Based on a typical core with a diameter of 32.6 centimeters the following core characteristics were calculated: a median fission energy in the core of 0.35 MeV, a prompt-neutron lifetime of 0.3 microsecond, and flux values of 8×10^{13} neutrons per square centimeter per second at the core center and 4×10^{13} neutrons per square centimeter per second at the core edge.

7. The parametric data are combined into design curves relating core diameter to required fuel density. Three curves, one each for the power-flattened condition of

radial peak- to average-power ratios of 1.05, 1.1, and 1.35 (unzoned), were constructed for a cylindrical core with a 0.95-centimeter W-25Re pressure vessel, 1.27-centimeter W end plates, and a 7.62-centimeter BeO radial reflector.

Lewis Research Center,
National Aeronautics and Space Administration,
Cleveland, Ohio, June 26, 1968,
120-27-06-05-22.

APPENDIX A

CROSS SECTIONS

Of the multigroup reactor codes available, the transport codes (such as the one-dimensional DTF and the two-dimensional TDSN) are particularly adaptable to small fast-spectrum cores. Also, the running time of DTF is sufficiently fast to permit parametric studies. However, before reactor calculations can be made it is necessary to obtain a set of neutron cross sections for the materials of interest. To accomplish this the GAM-II code was used to calculate P_0 and P_1 microscopic cross sections for 14 neutron energy groups from 15 MeV to 0.414 eV averaged over a fast flux spectrum. The spectrum was generated by GAM-II in a medium composed of a nominal core composition, and the group energy split was similar to the Hansen-Roach cross-section set (ref. 21). Because of the importance of inelastic scattering in fast cores, the full-down scattering matrix in the GAM output was retained in the cross-section set. Also, a resonance calculation was performed to refine the spectrum in the eV to keV range. The energy range below 0.414 eV was divided into two groups, and the cross sections were either generated by TEMPEST-II or hand calculated. No effort was made to refine these relatively rough values for the two low-energy regions because of their relative unimportance to fast-reactor calculations. In addition, a set of Be cross sections was generated which were flux weighted over a moderating medium (BeO) spectrum. These cross sections were used in the reactor reflector regions.

An initial check on the validity of the cross section was made by calculating a number of critical assemblies (table X). These assemblies were selected because of their size and the similarity of materials to those expected to be used in this study. All cases were calculated with P_0 transport-corrected cross sections, and the results were sufficiently close to $k = 1.0$ to warrant confidence in their accuracy. The fact that all values (except the 710 critical) exceeded 1 is characteristic of the use of P_0 transport-corrected cross sections. The low value of the 710 calculation probably is the result of a discrepancy in the transverse leakage.

A more comprehensive check on the cross sections and the use of DTF was obtained by comparison of flux and power distribution calculations with 710 critical experiment data. (Although specific data on this experiment are classified, it is similar to the model described in reference 20.) Values dependent on a fast spectrum (central core region) were accurate, whereas those near the core edge (which were more dependent on low-energy neutrons) showed more deviation. At the core center the fission ratio of U^{238} to U^{235} was underpredicted by 2.3 percent and the local- to minimum-power ratio was overpredicted by 10 percent, whereas at the core edge the local- to minimum-power ratio was underpredicted by 29 percent.

TABLE X. - CRITICAL EXPERIMENT CALCULATIONS

Core	Calculated multiplication constant, k	Comments
Godiva	1.012	Small bare sphere of 93.9 percent enriched U (ref. 21)
Be-reflected sphere	1.042	Small sphere of 93.5 percent enriched U surrounded by a 5.08-cm Be shell (ref. 21)
W-diluted bare sphere	1.000	Bare sphere composed of 0.309 enriched U and 0.691 W (ref. 22)
W-diluted bare sphere	1.014	Bare sphere composed of 0.5 enriched U and 0.5 W (ref. 23)
Ta-diluted bare sphere	1.029	Bare sphere composed of 0.495 enriched U and 0.505 Ta (ref. 23)
W-reflected sphere	1.009	Small sphere of 93.5 percent enriched U surrounded by a 10.16-cm W shell (ref. 21)
710 critical experiment	.989	Cylinder composed of 0.27 enriched U, 0.26 W, 0.1 Ta, and 0.1 Al with a 15-cm Be radial reflector (transverse leakage was estimated from a 2-D calculation) (ref. 20)

However, since overall reactor properties in these small, fast cores are primarily dependent on fast spectrum properties, both the calculational method and the cross sections appeared adequate for this study. An interesting aspect of the critical experiment data was the spectrum in the Be reflector region as defined by cadmium (Cd) ratios from foil experiments. Criticality calculations indicated that both the multiplication constant of the system and the spectrum in the Be region could be varied by separating the Be into two regions, one in which fast-spectrum-averaged cross-sections were used and one in which moderating spectrum cross sections were used.

This division would seem logical since the fast spectrum from the core is slowed down (moderated) considerably by the Be, the degree of moderation being dependent on the depth of penetration. The use of Be fast cross sections over the entire Be region resulted in a larger multiplication constant and a lower Cd ratio. A calculation using Be fast cross sections for the first 4.14 centimeters and Be moderated cross sections for the remainder of the Be region gave a closer approximation to the experimentally determined Cd ratios. However, these were slightly high and it was decided to use Be fast cross sections over the first 5.08 centimeters of the reflector region (BeO) and Be moderated cross sections for the remainder for the parametric calculations in this

TABLE XI. - DEPENDENCE OF DTF CALCULATIONS ON
INPUT OPTION

Input option comparison	Reactivity change, ^a percent reactivity
S ₄ - S ₆	0.15
^b P ₀ - P ₁	1.4
Convergence criterion, case with 1×10 ⁻⁴ - case with 1×10 ⁻⁵	0
Be cross sections, case with moderated ^c - case with fast ^c	-1.5
Cross sections, case with resonance corrected - case with nonresonance ^d	1.2

^aBased on criticality calculations of 710 critical experiment.

^bTransport-corrected P₀ cross sections.

^cType of spectrum weighting in GAM-II calculation.

^dIn a nonresonance calculation GAM-II uses a resonance integral for calculating cross sections.

design study. The effect of Be cross sections on the multiplication constant is indicated in table XI.

APPENDIX B

CALCULATION TECHNIQUES

A few of the options in the use of DTF were investigated prior to undertaking parametric criticality calculations (table XI). Based on these results all reactor calculations were made using the transport-corrected P_0S_4 code option with a convergence criteria of 1×10^{-4} and resonance-corrected cross sections. Although this procedure indicates that multiplication constants could be overpredicted by 1.55 percent Δk , the low value calculated for the 710 critical experiment (-1.1 percent Δk in table X) represents a counteracting correction. Therefore, multiplication constants were reported in this study as calculated.

The calculation model used homogenized regions in cylindrical geometry and, for one-dimensional problems, a buckling to simulate transverse leakage. The buckling is calculated internally in DTF by using an extrapolated dimension; for example, for axial leakage from a cylinder this equals the actual height plus reflector savings plus twice an extrapolation length of $0.71/\Sigma_{tr}$.

REFERENCES

1. Stewart, Warner L.; Anderson, William J.; Bernatowicz, Daniel T.; Guentert, Donald C.; Packe, Donald R.; and Rohlik, Harold E.: Brayton Cycle Technology. Space Power Systems Advanced Technology Conference. NASA SP-131, 1966, pp. 95-145.
2. Lubarsky, Bernard; and Shure, Lloyd I.: Applications of Power Systems to Specific Missions. Space Power Systems Advanced Technology Conference. NASA SP-131, 1966, pp. 269-285.
3. Freedman, S. I.; Keiser, J. T.; Cohen R. M.; and Terrill, W. R.: Nuclear Brayton Cycle Powerplants for Space Applications. Advances in Energy Conversion Engineering. ASME, 1967, pp. 749-769.
4. Whitmarsh, Charles L., Jr.; and Kerwin, Paul T.: A 1-Megawatt Reactor Design for Brayton-Cycle Space Power Application. I - Thermal Analysis and Core Design. NASA TN D-5013, 1968.
5. Whitmarsh, C. L., Jr.: Reactivity Effects Caused by Radial Power Flattening in a Small, Fast-Spectrum Reactor. NASA TN D-4459, 1968.
6. Mondt, Jack F.: The Design Analysis of a 100-Kilowatt Gas Cooled Reactor. M. S. Thesis, Univ. Washington, 1965.
7. Blinn, H. O., et. al.: High-Temperature Liquid-Metal-Cooled Reactor-Phase I. Vol. I. Rep. WANL-PR (R)-002, Westinghouse Electric Corp., Mar. 1964.
8. Gronroos, H. G.: Criticality Calculations for a Fast Liquid-Metal-Cooled Reactor - Phase I. Tech. Rep. 32-512, Jet Propulsion Lab., California Inst. Tech. (NASA CR-53017), Nov. 15, 1963.
9. Rosenblum, Louis; Englund, David R., Jr.; Hall, Robert W.; Moss, Thomas A.; and Scheuermann, Coulson: Potassium Rankine System Materials Technology. Space Power Systems Advanced Technology Conference. NASA SP-131, 1966, pp. 169-199.
10. Martin, F. S.; and Ainscough, J. B.: Uranium Dioxide Fuel, An Assessment of Selected Data. TRG Report 681(S), United Kingdom Atomic Energy Authority, Apr. 1965.
11. Bugl, J.; and Keller, D. L.: Uranium Mononitride - A New Reactor Fuel. Nucleonics, vol. 22, no. 9, Sept. 1964, pp. 66-70.
12. Anon.: High-Temperature Materials and Reactor Component Development Programs. Volume I. Materials. Rep. GEMP-177A, General Electric Co., Feb. 28, 1963.

13. Carlson, B. G.; Worlton, W. J.; Guber, W.; and Shapiro, M.: DTF Users Manual. Vol. I, UNC Phys/Math-3321, United Nuclear Corp., Nov. 1963.
14. Barber, Clayton E.: A Fortran IV Two-Dimensional Discrete Angular Segmentation Transport Program. NASA TN D-3573, 1966.
15. Joanou, G. D.; and Dudek, J. S.: GAM-II. A B₃ Code for the Calculation of Fast-Neutron Spectra and Associated Multigroup Constants. Rep. GA-4265, General Atomic Div., General Dynamics Corp., Sept. 16, 1963.
16. Shudde, R. H.; and Dyer, J.: TEMPEST-II, A Neutron Thermalization Code. Rep. TID-18284, Atomics International, June 1962.
17. Meghreblian, Robert V.; and Holmes, David K.: Reactor Analysis. McGraw-Hill Book Co., Inc., 1960, p. 763-780.
18. Brehm, Richard L.: Estimates of Doppler Coefficients for In-Pile Thermionic Reactor Materials. Tech. Rep. 32-1077, Jet Propulsion Lab., California Inst. Tech. (NASA CR-85358), Oct. 1, 1967.
19. Keepin, G. Robert: Physics of Nuclear Kinetics. Addison-Wesley Publ. Co., Inc., 1965.
20. Petersen, G. T.; Kunze, J. F.; Wall, J. B.; Hallam, J. W.; Henderson, W. B.; and Warzek, F. G.: Recent Fast Critical Experiments in the MSCA and 710-CE. Proceedings of the International Conference on Fast Critical Experiments and Their Analysis. Rep. ANL-7320, Argonne National Lab., 1966, pp. 1950203.
21. Staff of Argonne National Lab.: Reactor Physics Constants. Rep. ANL-5800, 2nd ed., Argonne National Lab., July 1963, p. 585.
22. Cohn, C.; Golden, G.; Hogle, B.; Loewenstein, W.; Rosenberg, G.; Sparks, D.; and Youngdahl, C.: Basic Material Resulting from ANL Rocket Study. Rep. ANL-6656, Argonne National Lab., May 1963.
23. Paxton, H. C.; Thomas, J. T.; Calliham, Dixon; and Johnson, E. B.: U²³⁵, Pu²³⁹ and U²³³. Rep. TID-7028, Los Alamos Scientific Lab., June 1964.